Experimental quality factor determination of guided-mode resonances in photonic crystal slabs

Yousef Nazirizadeh,[1,a] Uli Lemmer,[1] and Martina Gerken[2]
[1]*Light Technology Institute, Universität Karlsruhe (TH), Kaiserstr. 12, D-76131 Karlsruhe, Germany*
[2]*Institute of Electrical and Information Engineering, Christian-Albrechts-Universität Kiel, Kaiserstr. 2, D-24143 Kiel, Germany*

(Received 10 November 2008; accepted 6 December 2008; published online 29 December 2008)

We report on a method how quality factors of guided-mode resonances in photonic crystal slabs (PCSs) can be determined in the reciprocal space. Transmission measurements through PCSs are performed using crossed polarization filters before and after the PCS. Consequently the unwanted illumination source is suppressed and only the guided-mode resonances are revealed. This method allows for a spatially resolved quality factor determination in the reciprocal space. As an example we scan a two-dimensional PCS and visualize its inhomogeneities. Although the resonance wavelength variations were only ≈3 nm, the quality factor varies from 100 to 350. © *2008 American Institute of Physics*. [DOI: 10.1063/1.3058682]

Photonic crystal slabs (PCSs) are one of the most promising nanostructures for optical and optoelectronic devices. The quality (Q) factors of modes provided by such structures are important design parameters, which define how long light is captured by the PCS and can interact with the device. Two mechanisms are responsible for the light confinement in PCSs in all spatial directions: horizontal confinement by the two-dimensional photonic crystal and vertical confinement by the high refractive index contrast. Modes, which have no radiation components to the far field due to total internal reflection, are called *guided modes*. Modes that lie above the light line and thus couple to far field radiation are referred to as *guided-mode resonances* (GMRs). The Q-factor of a GMR is limited by its leaky component to far field radiation. In terms of applications, high Q-factor GMRs may be utilized for distributed feedback (DFB) lasers[1,2] or narrow bandwidth bandpass filters.[3] In contrast, GMRs with low Q-factor may be used for light extraction out of light emitting diodes.[4,5]

In previous investigations the linewidths of GMRs have been studied in the reciprocal space.[6,7] However, the used methods provided a lower limit on the resolvable linewidth and hence showed disagreements comparing theory with experimental results. Many theoretical models are known for calculating losses of GMRs[8–11] that can be used to calculate its Q-factor. For real PCSs, however, the Q-factor is strongly affected by geometric parameters such as hole depth and shape.[12] Therefore, experimental characterization is an essential procedure. The luminescence spectra of a proper emitting layer inside the PCS will reveal the GMRs, which have a Lorentzian line shape.[13] From these spectra the Q-factor can be determined by applying the corresponding fit procedure. Determining the Q-factor in passive PCSs is performed by analyzing the transmission and reflection spectra using a white-light source.[14] Here the spectrum is a superposition of the light source, which experiences thin-film effects and the GMRs. To obtain the Q-factor, an Airy–Fano model is necessary for the fitting procedure. In this paper we propose to use transmission measurements with two crossed polarization filters, before and behind the PCS, to suppress the light source, which allows the direct observation of the GMRs with Lorentzian line shape.[15] This requires a pure Lorentzian fit procedure for the Q-factor determination, which is easy to implement. Moreover this method can be performed in the absence of emitting materials in the PCS.

Throughout this work we used a confocal microscope setup for the angle resolved and spatially resolved transmission measurements. As shown in Fig. 1(a) a halogen lamp in combination with a condenser is used for the illumination. In the detection arm, an objective with a magnification of 40× and a pinhole with 100 μm diameter deliver 2.5 μm spatial resolution on the PCS. Two crossed polarization filters with an extinction ratio of 8500:1 are placed before (polarizer) and after (analyzer) the PCS. A variable slit diaphragm defines the polar angle range from 3° to θ for the illumination. Transmission measurement at a particular polar angle θ is generated by opening the slit diaphragm incrementally and subtracting consecutive results. All presented investigations are performed on a PCS, which is a 221 nm Nb_2O_5 layer (n=2.3 for wavelength λ=500 nm) on a quartz substrate with holes in a hexagonal geometry and a periodicity of 360 nm. This structure was fabricated by an electron beam lithography and a dry etching process.[16] Figure 1(b) shows a scanning electron microscope (SEM) image of the PCS, which was cut by a focused ion beam. In the cross section a

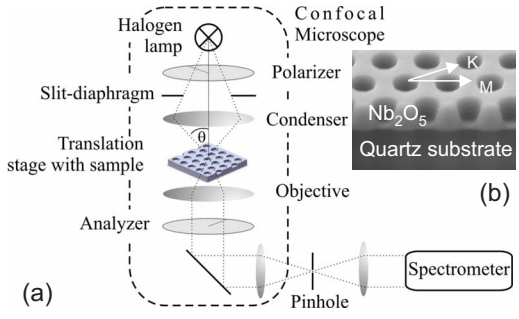

FIG. 1. (Color online) (a) Confocal microscope setup for angle resolved transmission measurements with orthogonally oriented polarization filters. (b) SEM image of PCS cut with focused ion beam. Holes show a noncylindrical profile.

[a]Electronic mail: yousef.nazirizadeh@lti.uni-karlsruhe.de.

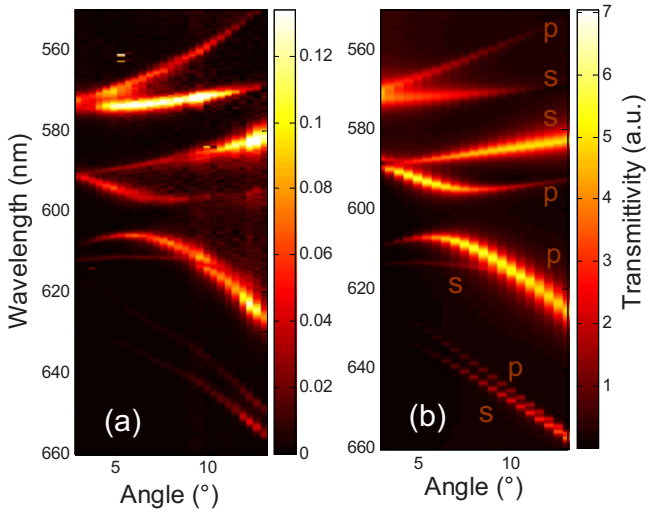

FIG. 2. (Color online) (a) Transmittivity of PCS in the Γ-*M* direction using crossed polarization filters. Only GMRs with Lorentzian line shape are transmitted. (b) Transmittivity 3D FDTD simulation for *s*- and *p*-polarized lights. The letters *s* and *p* indicate the polarization of the particular modes.

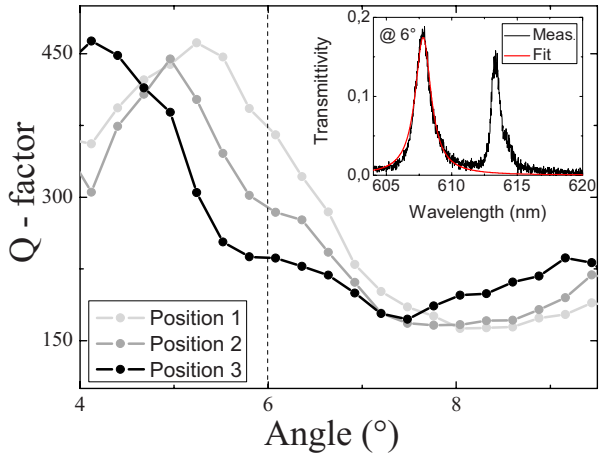

FIG. 3. (Color online) *Q*-factor angular dependency of the fourth mode from the bottom in Fig. 2(a) at three positions on the PCS. The maximum of the *Q*-factor shifts to lower angles moving toward the edge of the PCS field. Inset: transmission spectra at 6° with the corresponding fitted curve.

noncylindrical hole shape is observed, which is not patterned fully into the Nb_2O_5 layer.

In Fig. 2(a) transmission measurements from 3° to 13° in the Γ-*M* direction are shown. The transmission measurements are normalized to the spectrum measured with parallel polarization filters and no sample. As we use free-space illumination, only modes above the light line are excited. Hence, the transmission spectra that are recorded follow the band structure of the PCS above the light line. Due to the crossed polarization filters the light, which is not interacting with the PCS, is suppressed, which results in a Lorentzian line shape for the GMRs. The variety and the angular dependency of the GMR linewidth are clearly visible. Photonic crystal modes with a high *Q*-factor, which have a small linewidth, will have a low coupling to the far field modes. Thus, in transmission measurements excitation of these modes and outcoupling again to far field modes are inefficient and these modes appear darker. For the same reason modes with a low *Q*-factor appear brighter.

To verify these results we performed three-dimensional (3D) transmission simulations using the finite-difference time-domain (FDTD) method. The computational domain is a single unit cell of the PCS. As the correct shape of PCS holes is critical for these calculations, we described the shape of the hole using a polynomial function adapted to the cross section of the PCS shown in Fig. 1(b). The slab thickness and the real and imaginary parts of the refractive index of Nb_2O_5 were determined by transmission measurement of unstructured regions. The region below the PCS was filled with quartz glass as a substrate material. At the top and bottom of the simulation cell, perfectly matched layer absorbing boundary conditions were imposed. For the remaining surfaces we imposed Bloch periodic boundary conditions to ensure the periodicity of the PCS. A plane wave source placed before the PCS was used as illumination source. This plane wave source generates a short electromagnetic pulse, allowing a broadband excitation in a single run. A monitor point was placed after the PCS to record the field amplitude. By Fourier transforming the recorded signal, the transmission spectra through the PCS were obtained. The simulation duration was 3000 fs. In the first 110 fs of the simulation both the direct transmission of electromagnetic waves without interaction with the PCS as well as light interacting with the PCS are recorded. In the remainder of the simulation time GMRs are recorded. Depending on the lifetime of the GMRs the transmission of the electromagnetic wave is delayed. Thus, by filtering out the first 110 fs of the recorded field amplitude only the GMRs are visible.[8] In Fig. 2(b) transmission simulations from 3° to 13° for *s*- and *p*-polarizations are shown. We see a good agreement comparing the experiment and simulated results, both in resonance position and linewidth.

In the following we investigate the fourth mode from the bottom in Fig. 2(a) regarding its *Q*-factor. For this purpose measurements were performed with higher accuracy to ensure better conditions for the *Q*-factor determination process. We minimized the difference between the measured spectra at a particular angle and a Lorentzian function to find the linewidth of the resonances (inset in Fig. 3). This linewidth is converted into the *Q*-factor of the GMR under investigation. Figure 3 (position 1) presents the angular evolution of the *Q*-factor, which shows a maximum at about 5° with a value of 450. For higher angles the *Q*-factor drops down to 150. Recently a DFB laser was shown[17] with laser action at 3°. This was explained by the *Q*-factor of the GMR contributing to the laser action. It was shown theoretically that this mode has a maximum in *Q*-factor at around 3°. Our results deliver an experimental evidence for this behavior.

During the fabrication process, parameters can drift, which results in a drift in geometric parameters. As the *Q*-factor of GMRs is strongly affected by these parameters small drifts can significantly change the *Q*-factor. Using SEM images, such small parameter drifts cannot be distinguished. To overcome this problem we perform spatially and angle resolved *Q*-factor measurements. In Fig. 3 the *Q*-factor angular evolution is shown for three positions near the edge of the PCS field. The distance between two measurement points is 4 μm. The maximum of the *Q*-factor shifts to lower angles when approaching the PCS field edge. To map the homogeneity of the PCS we performed a transmission scan at 6°. For this scan we used an additional 1.5× magnification lens in the detection arm to increase the spatial res-

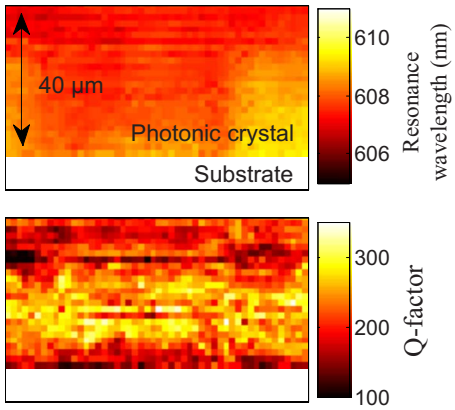

FIG. 4. (Color online) Transmittivity scan at 6° around the edge of the PCS field. Resonance wavelength and Q-factor of the fourth mode are shown. Although no significant changes in resonance wavelength are observed, the Q-factor shows large variations.

olution to approximately 1.6 μm. At this particular angle the highest variation in Q-factor is expected from Fig. 3. The resonance wavelength and the Q-factor obtained by the fitting procedure are shown in Fig. 4. While the resonance wavelength varies from 607 to 609 nm ($<0.5\%$), we observe for the Q-factor a lowering from 350 down to 100 ($\approx 70\%$). With this method small geometric variations, which can affect the fundamental functionality of optoelectronic devices, can be visualized.

In conclusion, we presented a method for angular and spatially resolved Q-factor measurements using crossed polarization filters. We showed spatially resolved band structure measurements for a Nb_2O_5 PCS with hexagonal geometry. Corresponding FDTD simulations showed good agreements with the experimental results. To investigate the inhomogeneities of the PCS we performed spatially resolved scans, while small variations were observed in resonance wavelength, the Q-factor varies up to 70%.

We thank D. Schelle, E. Kley, and A. Tünnermann of the Institute of Applied Physics at the Friedrich-Schiller University Jena for providing the sample photonic crystal slab. Furthermore, we acknowledge the support from the German Federal Ministry for Education and Research BMBF (Project No. 03X5514).

[1] S. Wang and S. Sheem, Appl. Phys. Lett. **22**, 460 (1973).
[2] M. Meier, A. Mekis, A. Dodabalapur, A. Timko, R. E. Slusher, J. D. Joannopoulos, and O. Nalamasu, Appl. Phys. Lett. **74**, 7 (1999).
[3] Y. Ding and R. Magnusson, Opt. Express **12**, 5661 (2004).
[4] S. Fan, P. R. Villeneuve, J. D. Jannopoulos, and E. F. Schubert, Phys. Rev. Lett. **78**, 3294 (1997).
[5] K. Ishihara, M. Fujita, I. Matsubara, T. Asano, and S. Noda, Appl. Phys. Lett. **90**, 111114 (2007).
[6] V. Pacradouni, W. J. Mandeville, A. R. Cowan, P. Paddon, J. F. Young, and S. R. Johnson, Phys. Rev. B **62**, 4204 (2000).
[7] M. Galli, D. Bajoni, M. Belotti, F. Paleari, M. Patrini, G. Guizzetti, D. Gerace, M. Agio, L. C. Andreani, D. Peyrade, and Y. Chen, IEEE J. Sel. Areas Commun. **23**, 1402 (2005).
[8] S. Fan and J. D. Joannopoulos, Phys. Rev. B **65**, 235112 (2002).
[9] L. C. Andreani and D. Gerace, Phys. Rev. B **73**, 235114 (2006).
[10] A. R. Cowan, P. Paddon, V. Pacradouni, and J. F. Young, J. Opt. Soc. Am. A **18**, 1160 (2001).
[11] T. Ochiai and K. Sakoda, Phys. Rev. B **63**, 125107 (2001).
[12] R. Ferrini, R. Houdré, H. Benisty, M. Qiu, and J. Moosburger, J. Opt. Soc. Am. B **20**, 469 (2003).
[13] G. A. Turnbull, P. Andrew, W. L. Barnes, and I. D. W. Samuel, Phys. Rev. B **67**, 165107 (2003).
[14] K. B. Crozier, V. Lousse, O. Kilic, S. Kim, S. Fan, and O. Solgaard, Phys. Rev. B **73**, 115126 (2006).
[15] Y. Nazirizadeh, J. Müller, U. Geyer, D. Schelle, E. Kley, A. Tünnermann, U. Lemmer, and M. Gerken, Opt. Express **16**, 7153 (2008).
[16] M. Augustin, H.-J. Fuchs, D. Schelle, E.-B. Kley, S. Nolte, A. Tünnermann, R. Iliew, C. Etrich, U. Peschel, and F. Lederer, Opt. Express **11**, 3284 (2003).
[17] K. Forberich, M. Diem, J. Crewett, U. Lemmer, A. Gombert, and K. Busch, Appl. Phys. B: Lasers Opt. **82**, 539 (2006).